

# Optimisation of the $f/2$ Gemini focal spot using full beam adaptive optics

Contact [dan.symes@stfc.ac.uk](mailto:dan.symes@stfc.ac.uk)

C. D. Gregory, D. R. Symes, M. Baraclough, T. Anderson, S. J. Hawkes, C. J. Hooker, O. Chekhlov, B. Parry, Y. Tang, N. Booth, P. S. Foster, P. P. Rajeev

Central Laser Facility, STFC Rutherford Appleton Laboratory, Chilton, Didcot, OX11 0QX, UK

## Introduction

For optimum performance of the Gemini laser system it is critical to maintain a high quality focal spot in order to reach the highest possible intensities. In our previous paper [1] we reported that we have installed adaptive optics in both beamlines to compensate for aberrations present in the laser wavefront. Here we detail the method we have adopted for routine optimisation of the adaptive optic for the  $f/2$  focusing option.

## Full-size adaptive optics

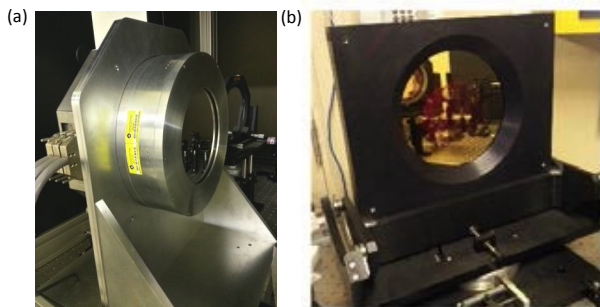


Figure 1. Photographs of full-beam adaptive optics which use (a) mechanical and (b) piezoelectric actuators.

There are two adaptive optics (AOs) available for the full size (150mm diameter) beam in Gemini TA3 (See Fig. 1). The first (CLF AO) was constructed in-house and uses 61 piezoelectric actuators to deform the mirror surface. Piezoelectric actuators have the advantage of a fast response so that optimisation can be done quickly. In addition the spot can be manually adjusted in real-time while imaging the focus, due to the almost instantaneous response of the mirror. The second optic (ILAO) is a commercial product from Imagine Optic [2] that uses 52 mechanical actuators. This allows a far larger stroke that can correct up to 100 waves of aberration, but functions more slowly than the CLF AO. This means it is difficult to manipulate the focal spot manually unless the required change is known. The ILAO has a dielectric high-reflectivity coating and the CLF AO has a gold coating. We intend to introduce a replacement piezoelectric AO with a dielectric coating in the near future.

The AO is optimised by measuring the wavefront of the beam using an Imagine Optic HASO wavefront sensor and driving the mirror with the CASAO software package. After obtaining an interaction matrix that determines the effect of each actuator in turn, the software calculates the actuator pattern needed to minimise the aberration in the beam. This process takes a few minutes with the CLF AO but can take up to 30 minutes with the ILAO because of its slower response.

## Optical arrangement for AO optimisation

We measure the Gemini wavefront after the final focusing optic so that aberrations due to this optic are also corrected. Ideally the transport optics for the HASO should image the AO at the

plane of the detector for the optimum performance. This is straightforward with the  $f/20$  parabola: a wedge is inserted into the beamline to steer the beam out of the vacuum chamber through a 1mm thick window, and the beam is re-collimated at the correct size for the HASO with a 70mm focal length lens.

For the  $f/2$  focusing beam we have adapted the focal spot camera to allow simultaneous measurement of the focal spot and the wavefront (see Fig. 2). To image the focus we use a 50x magnification, infinity-corrected microscope objective followed by a secondary (tube) lens of focal length 200mm. This arrangement allows us to use additional optics in the imaging path after the objective lens [3]. As shown in Fig. 2, we have three beamsplitters between the objective lens and the tube lens allowing the back of the target to be illuminated with an LED and a laser light source for positioning (see D. R. Symes *et al.*, also in this CLF Annual Report). We use the beam transmitted through the first beamsplitter to measure the wavefront. An image of the AO is formed several millimetres from the rear of the objective. This can be re-imaged with a lens of focal length 30mm to a plane approximately 200mm behind the beamsplitter, with a beamsize well matched to the HASO sensor.

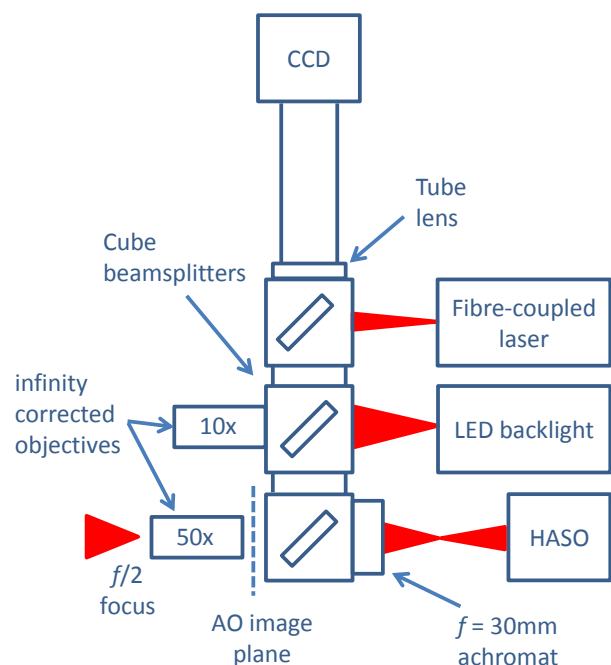
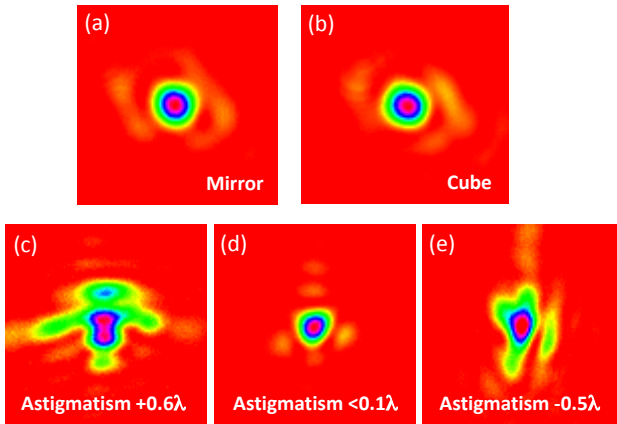


Figure 2. Camera arrangement used for simultaneous measurement of focal spot and wavefront.

We ensured that the use of a beamsplitter did not introduce any significant aberration to the measurement by imaging the focal spot after reflections from a mirror (Fig. 3(a)) and from a beamsplitter (Fig. 3 (b)). We also checked that aberrations added with the AO were consistent with both the focal spot image and the HASO measurement of the Zernicke terms. For

example in Fig. 3(c – e) we show the focal spot as we introduce first positive and then negative astigmatism at 0 degrees using the ILAO in open-loop correction mode.



**Figure 3. Comparison of best focus using (a) a mirror and (b) a cube beamsplitter in the camera system. (c – e) The focal spot measured on the camera as the astigmatism is scanned using the AO.**

### Beam attenuation

One challenge of focal spot measurements is to attenuate the beam sufficiently to avoid damage to the objective lens and the camera. Gemini has four power modes available, the lowest of which provides  $\sim 0.5$  mJ into Target Area 3. The attenuation optics are located after the 10 Hz amplification stages, in order to maintain the same laser beam parameters through the first 3 amplifiers. In the laser area (LA2) there is also a half-waveplate followed by a polariser, which can reduce the beam energy by a factor of  $\sim 100$ . We have verified in separate measurements with the full power beam (to be reported at a later date) that the wavefront and focal spot are not affected by this attenuation scheme. However, the low power beam still contains significantly higher energy than can be handled by the objective lens and additional attenuation is therefore required.

Previously we have provided additional attenuation by sliding lens tissue into the beam in the laser area (LA3). This has the effect of scattering light out of the beam but maintaining the same focal spot. It is acceptable for visualising the shape of a focus (for optimising a parabola for example) but does not give a correct value for the amount of energy contained within the spot. The correct light level must therefore be achieved by a combination of the LA2 waveplate and a reflective neutral density filter placed in front of the objective lens. This has the disadvantage that the filter will shift the focal plane slightly and also it must be checked carefully not to introduce any aberrations. We are currently replacing the tissue attenuators in LA3 with high reflectivity mirrors in order to remove the need for the additional filter in the target area.

On the North beamline, attenuation can be achieved when the plasma mirrors [4] are being used. In this case the focal spot can be imaged using the gold alignment stripe at the edge of the plasma mirror with the LA3 attenuators in the beam. The substrate is then driven into position on the anti-reflection (AR) coated portion. Because the double AR reflection provides a high degree of attenuation ( $\sim 10^4$ ), further attenuation in LA3 is not necessary.

### Optimisation results

The AO was optimised with this improved method using the North continuous wave 808nm alignment beam. Initially the plasma mirror system was bypassed and the  $f/2$  parabola optimised by minimising astigmatism in the focal spot. This is shown in Fig. 4 (a) where a reasonably good spot has been achieved with radius ( $1/e^2$ ) of  $w_0=1.7\mu\text{m}$ . However, when the

camera is saturated (Fig. 4(b)) it is clear that the energy contained within this central spot is lower than optimal at  $\sim 53\%$  ( $1/e^2$ ). Operating the AO routine improves the shape of the spot and raises the encircled energy to  $\sim 71\%$ .

The plasma mirror beamline, consisting of two  $f/7$  parabolas, was then introduced. These parabolas are optimised by minimising astigmatism, the first parabola using a separate focal spot camera within the plasma mirror system, the second parabola by using the main beam focal spot camera. The simultaneous measurement of wavefront and focal spot has made this process much easier. As can be seen in Fig. 4(e) the initial spot from the plasma mirrors was poor. We corrected this again with the AO and achieved the focal spot shown in Fig. 4 (g) which has radius ( $1/e^2$ ) of  $w_0=1.6\mu\text{m}$ .

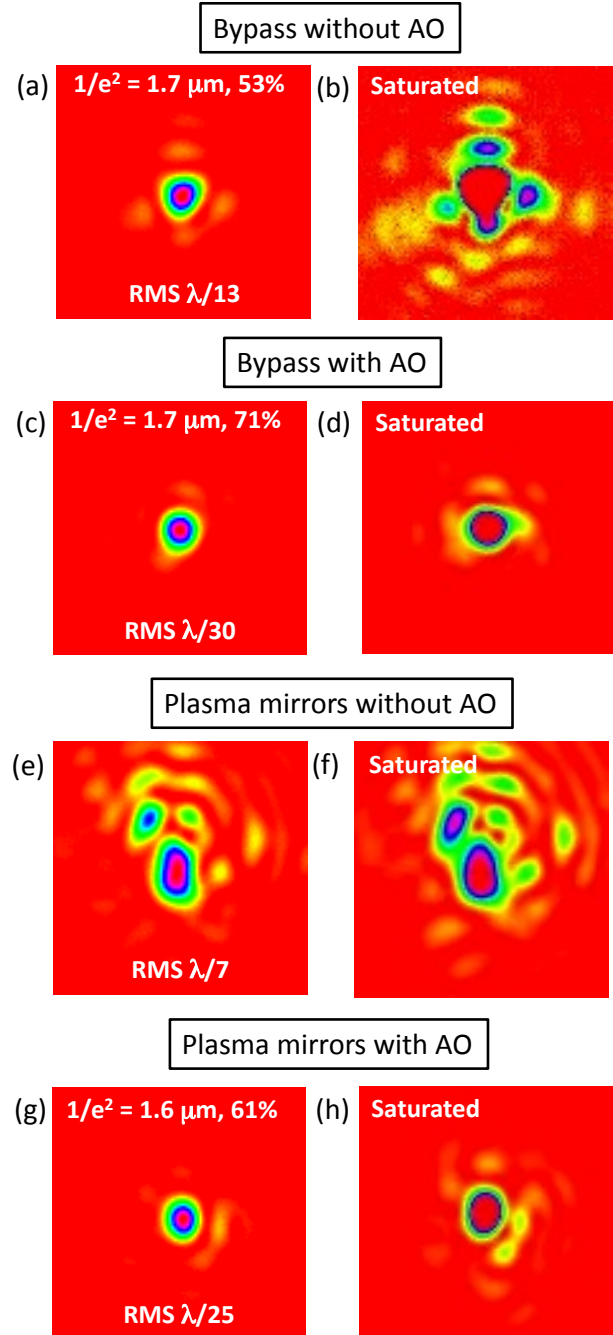


**Figure 4. Focal spots obtained with the  $f/2$  parabola with the CW alignment beam. (a – d) images with the plasma mirrors bypassed. (a) is without an adaptive optic (c) has an adaptive optic correction. (e – h) images including the plasma mirror system in the beamline (g) with and (e) without correction.**

The encircled energy is slightly lower (61%) than the bypass focus although further optimisation may be able to improve this.

The AO routine aims to make the wavefront as flat as possible and here has obtained better than  $\lambda/20$  RMS with and without plasma mirrors. The main Zernicke terms for a typical measurement are plotted in Fig. 5. Even with such a flat wavefront the encircled energy does not reach the theoretical maximum (76.6% for a top hat beam profile) and this may be caused by problems unrelated to the quality of the wavefront.

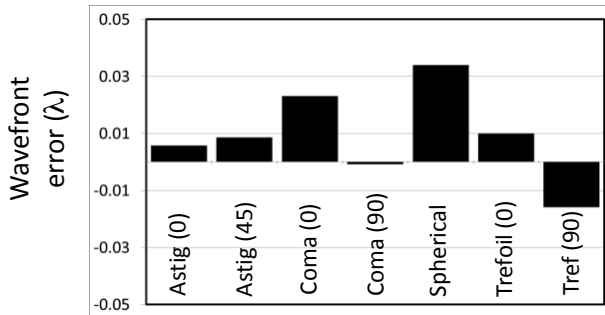


Figure 5. Wavefront achieved using ILAO and  $f/2$  parabola.

A further advantage of the AO is that it is now straightforward to switch between the plasma mirror and the bypass beamline. Recording separate actuator patterns for each beam avoids the need to match the differences in aberrations between them.

### Focal spot with the pulsed beam

The focal spot measurements shown in Fig. 4 were taken using the CW alignment beam, which is similar to the pulsed beam but not identical. Figure 6 shows a 12-bit image of the  $f/2$ , low-power focus after passing through the plasma mirror system. The  $(1/e^2)$  radius is  $w_0=1.6\mu\text{m}$ . We calculate an encircled energy within  $1/e^2$  of 58%, although as the image is slightly saturated this is an underestimate.

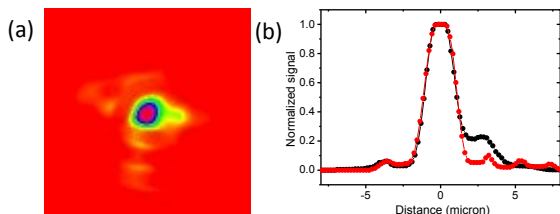


Figure 6. Focal spot of the pulsed beam using the ILAO and  $f/2$  parabola.

### Calculation of encircled energies

For analysis of the focal spots we have written an ImageJ [5] macro to estimate the  $1/e^2$  diameter. Beginning at the peak value of the image, a rectangular spiral-search moves outward and counts the number of pixels that have a value  $\geq 1/e^2$  of the peak value. The search terminates once a complete rectangle is traced with all values  $< 1/e^2$ , thus excluding any secondary peaks elsewhere in the image. The total area of the counted pixels is calculated, and the diameter of a circle of equivalent area is reported. There is also the option to calculate the D86 or  $D4\sigma$  values [6]. Taking the focal spot shown in Fig. 4(c), shown again in Fig. 7(a) and 7(b), we demonstrate the use of the macro to find the fraction of energy in a  $1/e^2$  diameter (Fig. 7(c)), the  $D4\sigma$  values (Fig. 7(d)) and the D86 radius (Fig. 7(e) and (f)).

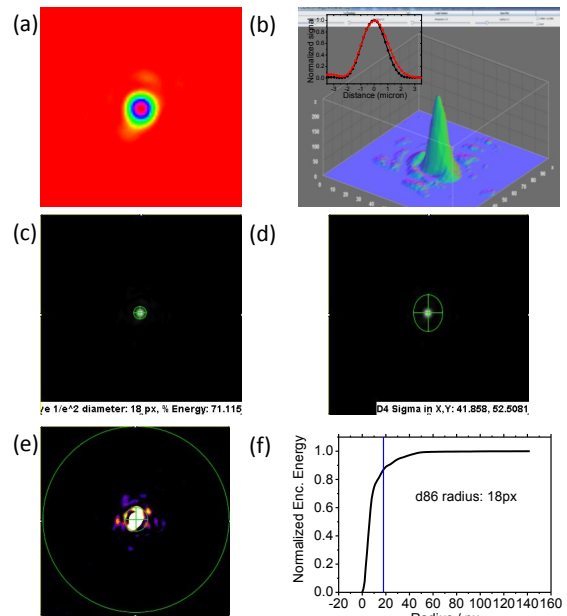


Figure 7. ImageJ macro used to read out focal spot diameters and encircled energy. Each pixel represents  $0.19\mu\text{m}$ .

### Conclusions

We have improved our implementation of adaptive optics on the  $f/2$  beamline on Gemini by measuring the wavefront after the focusing optic simultaneously with the focal spot. This allowed us to optimise the wavefront to better than  $\lambda/20$ . The energy within a  $1.6\mu\text{m}$   $1/e^2$  radius spot is greater than 58%.

### References

1. D. R. Symes *et al.*, *CLF Annual Report 2012-2013: Laser Science and Development - Astra Gemini*
2. [www.imagine-optic.com](http://www.imagine-optic.com)
3. <http://www.edmundoptics.co.uk/technical-resources-center/microscopy/using-tube-lenses-with-infinity-corrected-objectives/>
4. M. J. V. Streeter *et al.*, *CLF Annual Report 2008/2009 p. 225.*
5. <http://imagej.nih.gov/ij/>
6. [https://en.wikipedia.org/wiki/Beam\\_diameter](https://en.wikipedia.org/wiki/Beam_diameter)